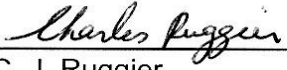


# 210 Delta Differential One-way Ranging

Released: July 15, 2004

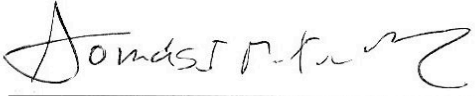
---

Document Owner:

  
\_\_\_\_\_  
C. J. Ruggier  
Tracking and Navigation  
System Engineer


6/28/04  
Date

Approved by:

  
\_\_\_\_\_  
T. J. Martin Mur  
Navigation Service Systems  
Development Engineer

6/29/04  
Date

Author:

  
\_\_\_\_\_  
P. W. Kinman

4/27/04  
Date

Released by:

Signature on File at DSMS Library  
\_\_\_\_\_  
DSMS Document Release

7/15/2004  
Date

***Change Log***

<b>Rev</b>	<b>Issue Date</b>	<b>Affected Paragraphs</b>	<b>Change Summary</b>
Initial	7/15/2004	All	New Module

***Note to Readers***

There are two sets of document histories in the 810-005 document that are reflected in the header at the top of the page. First, the overall document is periodically released as a revision when major changes affect a majority of the modules. For example, this document is part of Revision E. Second, the individual modules also change, starting as the initial issue that has no revision letter. When a module is changed, a change letter is appended to the module number on the second line of the header and a summary of the changes is entered in the module's change log.

## *Contents*

<u>Paragraph</u>	<u>Page</u>
1 Introduction .....	5
1.1 Purpose .....	5
1.2 Scope .....	5
2 General Information .....	5
2.1 Description of the Measurement .....	5
2.1.1 Differential One-Way Ranging .....	6
2.1.2 $\Delta$ DOR .....	7
2.1.3 DSN Equipment for $\Delta$ DOR Support .....	8
2.1.4 Data Acquisition .....	11
2.1.4.1 Example 1, Spacecraft With One DOR Tone and Subcarrier Harmonics .....	13
2.1.4.2 Example 2, Two Spacecraft With One DOR Tone and Subcarrier Harmonics .....	13
2.1.4.3 Example 3, Spacecraft With Only Subcarrier Harmonics .....	14
2.1.4.4 Example 4, Spacecraft With Uplinked Range Tone .....	14
2.2 Downlink Signal Structure and Power Allocation .....	15
2.2.1 DOR Tones and Phase Ambiguity .....	15
2.2.2 Downlink Power Allocation .....	17
2.2.2.1 One DOR Tone .....	18
2.2.2.2 Two DOR Tones .....	18
2.3 DOR Tone Signal-to-Noise Spectral Density Ratio .....	19
2.4 $\Delta$ DOR Measurement Error Models .....	20
2.4.1 Receiver Noise in DOR Tone Detection .....	20
2.4.2 Receiver Noise in Quasar Detection .....	21
2.4.3 Error in Knowledge of Quasar Position .....	21
2.4.4 Clock Instability .....	21
2.4.5 Instrumental Phase Ripple .....	22
2.4.6 Error in Knowledge of Station Location .....	22
2.4.7 Error in Knowledge of Earth Orientation .....	22
2.4.8 Troposphere .....	22
2.4.9 Ionosphere .....	23
2.4.10 Solar Plasma .....	23
2.5 $\Delta$ DOR Measurement Error Budget .....	23
References .....	25

## *Illustrations*

<b><u>Figure</u></b>	<b><u>Page</u></b>
1. Geometry of Differential One-Way Ranging.....	7
2. DSN Equipment for $\Delta$ DOR Support.....	9
3. Phase Ambiguity with One DOR Tone.....	16
4. Resolution of Phase Ambiguity with a Second DOR Tone .....	17

## *Tables*

<b><u>Tables</u></b>	<b><u>Page</u></b>
1. Microwave Sky Frequency Ranges for $\Delta$ DOR Tones .....	8
2. Supported Bandwidths and Resolutions with Resulting Data Rate .....	10
3. Channel Assignments for Example 1 .....	13
4. Channel Assignments for Example 2.....	13
5. Channel Assignments for Example 3.....	14
6. Channel Assignments for Example 4.....	14
7. Definition of $\alpha(\theta)$ and $\beta(\theta)$ for $\theta$ in peak radians .....	17
8. Example $\Delta$ DOR Error Budget.....	24
9. Parameter Values Associated with the Error Budget of Table 8.....	24

## ***1 Introduction***

### ***1.1 Purpose***

This module describes the capabilities and identifies the performance parameters for Delta-Differential One-way Ranging ( $\Delta$ DOR) measurements at the Deep Space Network (DSN) 34-m and 70-m stations.

### ***1.2 Scope***

The document provides information on the Delta-Differential One-way Ranging ( $\Delta$ DOR) technique. This document describes those parameters and operational considerations that are independent of the particular antennas being used. For antenna-dependent parameters, refer to the appropriate telecommunications interface module, modules 101, 103 and 104 of this handbook. The interpretation of any particular  $\Delta$ DOR measurement is dependent on the precise locations of the tracking antennas. Station locations are provided in module 301, Coverage and Geometry.  $\Delta$ DOR signals are received by the VLBI Science Receiver (VSR) that shares a common hardware design with the open-loop Radio Science Receiver (RSR) described in module 209. The quality of a  $\Delta$ DOR measurement depends on solar wind velocity that is discussed in module 106, Solar Corona and Solar Wind Effects.

## ***2 General Information***

Delta-Differential One-way Ranging is a radio-tracking technique that has proved very useful in the orbit determination of some spacecraft (References 1 and 2). It is an interferometric technique and therefore requires two Deep Space Stations located at different complexes for a single measurement.

### ***2.1 Description of the Measurement***

$\Delta$ DOR uses the differential one-way range technique to provide information about the angular location of a target spacecraft relative to a reference direction where the reference direction is defined by the direction of arrival of radio waves from a distant known source whose direction is well known. This is the origin of the “ $\Delta$ ” in the name “ $\Delta$ DOR”. The term *reference source* is applied to the distant source of radio waves that define the reference direction. Typically, the reference source is a quasar whose angular position in the sky is well known and cataloged, having been previously measured and studied. Sometimes, the reference source is a second spacecraft whose position in the sky is better known than that of the target spacecraft.

Since  $\Delta$ DOR provides a direct geometric determination of spacecraft angular position, it is especially useful for cases where line-of-sight measurements have weaknesses such as spacecraft near zero declination and spacecraft with small, unmodeled dynamic forces affecting their motion. It can also provide an independent cross-check of orbits determined by other methods and, in combination with these methods, can improve the accuracy of trajectory

determination.  $\Delta$ DOR measurements are of relatively short duration when compared to other orbit determination methods such as Doppler and two-way ranging (typically one hour or less compared with many hours). Thus, they can be used to reduce the total amount of tracking time necessary to attain the desired level of trajectory accuracy. The main disadvantages of  $\Delta$ DOR are that it requires two stations for each measurement and, in most cases, will disrupt telemetry when the reference source is being viewed.

### 2.1.1 *Differential One-Way Ranging*

The name, differential one-way ranging, comes from the fact that only a range difference, rather than an absolute range, is determined and that only the downlink is used. It is because only a range difference is being measured that it is possible to make this measurement one-way. (Absolute range measurement requires a highly-accurate clock at the target spacecraft as any clock error would translate directly into a range measurement error. This is the reason that ordinary ranging measurements send a ranging code derived from the station clock to the spacecraft, see modules 203 and 214.)

The geometry of differential one-way range is depicted in Figure 1. The radio waves from the target spacecraft arrive in approximately parallel rays at the interferometer. An imaginary line that connects the two antennas forming the interferometer is called the baseline and is denoted  $B$  in Figure 1. Since the antennas of the interferometer are located in different complexes on separate continents, the baseline  $B$  passes through the Earth. Also in Figure 1, an imaginary line segment  $L$  is drawn that is perpendicular to the arrival direction of the incoming rays. The shaded area around  $L$  represents the *a-priori* uncertainty in angle  $A$  and, because  $L$  is perpendicular to  $R$ , the uncertainty of the angle of the incoming radio waves with respect to the baseline. The interferometer measures the path length difference, also known as differential one-way range and indicated as  $\delta R$  in the figure. This enables the accuracy of  $A$  to be significantly improved. It is important to note that this is not a complete solution for the angular position in the sky of the target spacecraft. A single measurement only provides information about the location of the target spacecraft in the plane defined by the interferometer baseline and the target spacecraft.

The path length distance ( $\delta R$ ) is determined by recording the signals arriving at each station using an open-loop receiver. Later, when the signals from both stations are available at a common location, the two signals are correlated. The difference in group delay associated with the paths followed by the target spacecraft signal in propagating to the two stations is determined ( $\tau_g$ ) and converted into a path length difference by multiplying by the speed of electromagnetic waves in space ( $c$ ). The path length difference and knowledge of the baseline orientation is used to refine the angular position of the of the target spacecraft in the sky. The errors inherent in the DOR and  $\Delta$ DOR process are discussed in Paragraph 2.4. In discussing these errors, it is customary to use time units – that is, the units of differential group delay.

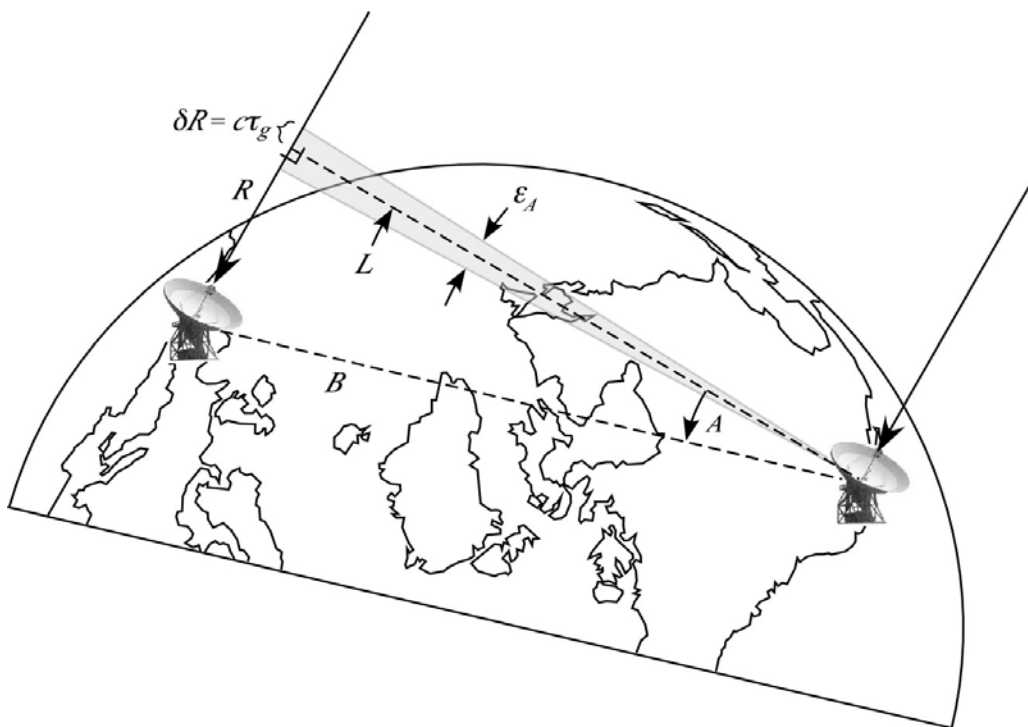


Figure 1. Geometry of Differential One-Way Ranging

( $B$  = Baseline;  $L$  = perpendicular to incoming rays;  $A$  = angle between  $B$  and  $L$ ;  
 $\delta R$  = differential one-way range,  $\epsilon_A$  = uncertainty in angle  $A$ )

The signals transmitted by the spacecraft should be high frequency, sinewave DOR tones to provide the best precision. Lower frequency subcarrier harmonics can be substituted for DOR tones, with some loss of precision, if DOR tones are not available. The subcarrier harmonics may be pure tones or spread by telemetry. The lowest possible symbol rate is preferred to reduce the squaring loss that occurs during signal processing. Uplinked range tones provide even less precision, but may be used if no other components are available. Subcarrier harmonics or additional DOR tones may also be required in order to resolve the phase ambiguity, see Paragraph 2.2.1.

### 2.1.2 $\Delta$ DOR

$\Delta$ DOR is a much more useful measurement for orbit determination than is plain DOR. In principle, a DOR measurement provides information about the angular position of the target spacecraft (within the plane of the interferometer plus target spacecraft). However, there are a number of measurement errors that prevent this form of measurement from being useful in the solution of the typical deep space orbit determination problem. The sources of these measurement errors are (among others) station clock offsets, instrumental group delays, and media effects. To calibrate these effects, a plain DOR measurement is made on a reference

source that is near the target spacecraft in an angular sense. The antennas are quickly moved to the target spacecraft and a similar measurement is made. Finally, the antennas are returned to the reference source to verify the calibration. This technique enables the effects of station clock offsets, instrumental group delay errors, and most of the media effects to be cancelled when the individual DOR results are differenced (which is a  $\Delta$ DOR measurement). The result is that the errors in a  $\Delta$ DOR measurement are much smaller than those for a plain DOR measurement and the technique becomes sufficiently accurate for orbit determination.

A number of missions have used  $\Delta$ DOR measurements as part of their orbit determination.  $\Delta$ DOR measurements played an important role in the orbit determination of 2001 Mars Odyssey (Reference 2) and the Mars Exploration Rovers (MER). Those  $\Delta$ DOR measurements were performed at X band. In the future,  $\Delta$ DOR measurements will also be performed in the Ka band for the Mars Reconnaissance Orbiter using beam-waveguide stations (Reference 3). The Ka-band stations that will support  $\Delta$ DOR are 25, 26, 34, 54 and 55. It should be noted that a VLBI measurement will always use two stations at different complexes, therefore stations 25 and 26 would not be used in the same measurement nor would stations 54 and 55. DSS 24 will have Ka-band capability but is not recommended for  $\Delta$ DOR because it has a less stable frequency reference for its downconverters.

### 2.1.3 *DSN Equipment for $\Delta$ DOR Support*

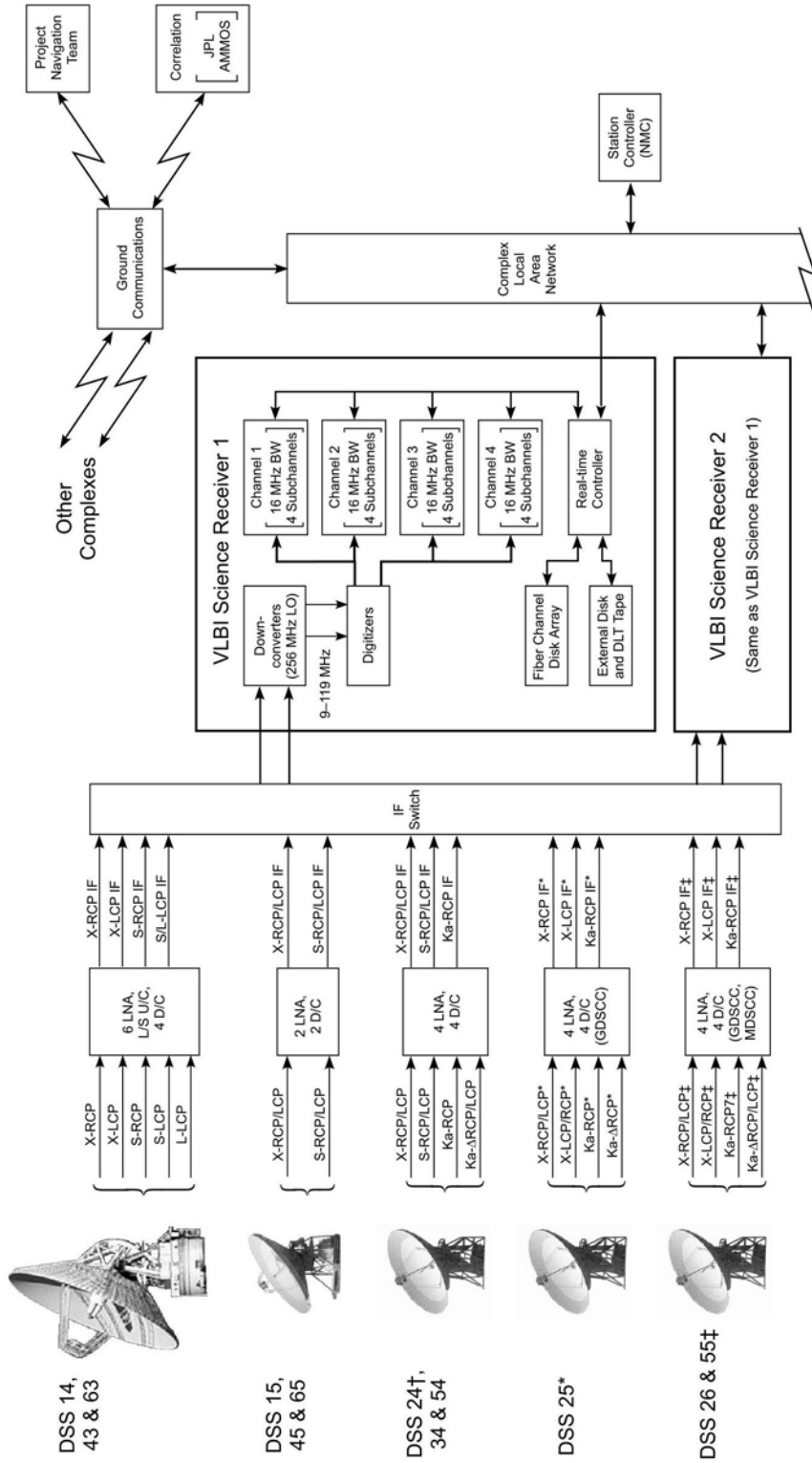
Differential one-way ranging is supported by the 34-m and 70-m antennas. Other equipment includes the VSRs in the complex Signal Processing Center (SPC), the ground communications infrastructure, and the DOR Correlator at JPL. Figure 2 depicts the DSN equipment used for  $\Delta$ DOR support.

The input to the VSR is one or two Intermediate-Frequency (IF) signals that have been downconverted from the microwave sky frequency, also referred to as the radio frequency (RF). The VLBI Science Receiver filters these IF signals, using a passband of 265-375 MHz. This is a fixed passband and, in combination with the RF to IF downconverters, places restrictions on the frequency ranges in which the  $\Delta$ DOR tones can be received. These restrictions, in terms of microwave sky frequency, are listed in Table 1. Additional restrictions based on the bandwidths of the antenna low noise amplifiers can be found in the Telecommunications Interface modules of this document.

Table 1. Microwave Sky Frequency Ranges for  $\Delta$ DOR Tones

Band	Acceptable Frequency Range	Remarks
S-band	2,265–2,375 MHz	Deep Space Allocation is 2,290–2,300 MHz
X-band	8,365–8,475 MHz	Deep Space Allocation is 8,400–8,450 MHz
Ka-band	31,965–32,075 MHz	Deep Space Allocation is 31,800–32,300 MHz





- \* Equipment or interface only exists at Goldstone DSSC
- ‡ Equipment or interface only exists at Goldstone and Madrid DSSCCs
- † DSS 24 is not recommended for ΔDOR measurements.

Figure 2. DSN Equipment for ΔDOR Support

The downconverted sky frequencies are further downconverted within the VSR to new IFs that span 9 – 119 MHz using a local oscillator of 256 MHz. These are digitized using a 256 MHz sampling clock, and the (8-bit) samples are sent to the Digital Downconverter (DDC). The DDC has two channels. Each selects a 16 MHz bandwidth from the original bandpass and downconverts it to baseband in the form of a 16 Ms/s, 8-bit, complex data stream. The center of each 16 MHz bandwidth can be set with a resolution of 1 MHz and optionally steered by predicts of the expected spacecraft sky frequency.

Each 16 MHz bandwidth can be further divided into two narrow-band and two wide-band subchannels centered around areas in the received spectrum that are useful in the DOR correlation process. Areas of interest may include the carrier, the DOR tones and their harmonics, and harmonics of subcarriers. The supported bandwidths and resolutions with the resultant data rate for each subchannel are listed in Table 2. The composite data rate for all selected subchannels at each of the two stations involved in the measurement must be routed to the  $\Delta$ DOR correlator at JPL for processing. This is a large amount of data and the capability of the ground communications infrastructure is often a key factor in determining the overall time required to complete a  $\Delta$ DOR measurement. At current effective transmission rates of about 2 Mb/s, (7.2 Gb/hr), four channels of 2-bit quantized quasar data with a 2 MHz bandwidth, and the associated narrower bandwidth channels for spacecraft signals, can be delivered to the correlator in near real-time assuming a 50 percent duty cycle between spacecraft and quasar measurements.

Table 2. Supported Bandwidths and Resolutions with Resulting Data Rate

Type Filter	Bandwidth	Resolution (bits per sample)	Resultant Data Rate (b/s)
Narrowband	1 kHz	16	32,000
	2 kHz	16	64,000
	4 kHz	16	128,000
	8 kHz	16	256,000
	16 kHz	16	512,000
	25 kHz	16	800,000
	50 kHz	16	1,600,000
	100 kHz	16	3,200,000
	1 kHz	8	16,000
	2 kHz	8	32,000
	4 kHz	8	64,000
	8 kHz	8	128,000

Table 2. Supported Bandwidths and Resolutions with Resulting Data Rate (Continued)

Type Filter	Bandwidth	Resolution (bits per sample)	Resultant Data Rate (b/s)
	16 kHz	8	256,000
	25 kHz	8	512,000
	50 kHz	8	800,000
	100 kHz	8	1,600,000
Wideband	1 MHz	8	16,000,000
	2 MHz	8	32,000,000
	4 MHz	8	64,000,000
	8 MHz	8	128,000,000
	16 MHz	8	256,000,000
	1 MHz	4	8,000,000
	2 MHz	4	16,000,000
	4 MHz	4	32,000,000
	8 MHz	4	64,000,000
	16 MHz	4	128,000,000
	1 MHz	2	4,000,000
	2 MHz	2	8,000,000
	4 MHz	2	16,000,000
	8 MHz	2	32,000,000
	16 MHz	2	64,000,000
	1 MHz	1	2,000,000
	2 MHz	1	4,000,000
	4 MHz	1	8,000,000
	8 MHz	1	16,000,000
	16 MHz	1	32,000,000

#### 2.1.4 *Data Acquisition*

$\Delta$ DOR measurements are conducted using either the Goldstone-Madrid baseline or the Goldstone-Canberra baseline. Two baselines with orthogonal components are needed to measure both the right ascension and declination coordinates of angular position. The Goldstone-Madrid baseline is oriented east-west and is most sensitive to right ascension for spacecraft near

the ecliptic plane. The Goldstone-Canberra baseline is canted and has most sensitivity in the direction that splits the axes of right ascension and declination. Since declination is usually the most difficult component of spacecraft state to extract from line-of-sight measurements, the Goldstone-Canberra baseline may provide information that cannot otherwise be obtained. The Goldstone-Madrid baseline is still useful to evaluate small dynamic force modeling and improve overall trajectory accuracy.

Planning a measurement involves scheduling the stations, selecting DOR tones or signal frequencies to be used, and identifying the appropriate reference source(s). Each VSR can process up to four tones or signals with its “narrow” channels (one tone or signal per channel). Next, the four VSR “wide” channels are assigned to record portions of the radio spectrum emitted from the reference source and centered about each narrow channel.

Narrow channels range in bandwidth from 1 to 100 kHz. Sample resolution of 1 to 16 bits may be selected. Channels are centered on the predicted received frequency of the spacecraft signal component to be recorded. Channel bandwidth must be chosen wide enough to include margin for errors in prediction of the spacecraft transmitter frequency and Doppler shift. Enough bits should be used to protect against radio frequency interference and avoid loss of Signal-to-Noise ratio. The spacecraft data volume is usually much smaller than the quasar data volume. As a result, a wider bandwidth or greater sampling resolution may be selected for the narrow channels without significantly increasing the total amount of data.

Quasar channels range from 1 to 16 MHz. A sample resolution of 1 to 2 bits is usually selected. Channel bandwidth must be chosen wide enough to provide sensitivity to detect the faint signals from extra-galactic radio sources that are used to calibrate the DSN as an interferometer. A channel bandwidth of 4 MHz with 2 bit samples is adequate to detect most of the sources in the JPL radio source catalog using a pair of DSN 34m antennas. A narrower bandwidth may be selected, and only stronger quasars observed, in order to reduce the volume of data that must be recorded.

To perform a measurement, the two Deep Space Stations forming the very long baseline interferometer make a series of observations to determine the differential one-way range to the target spacecraft and the reference source that preferably has a small angular separation from the target spacecraft. (Differential one-way ranging with a quasar is similar to what has been described above for a target spacecraft; however, there are important differences since the nature of the quasar “signal” is quite different from that of a spacecraft with DOR tones.) Each observation is referred to as a *scan*. In a typical  $\Delta$ DOR tracking pass of approximately one hour, the spacecraft and reference are alternately observed and a total of 5 to 10 scans, each lasting 5 to 10 minutes, are typically recorded. Some sources of measurement error can be reduced by making more observations, using shorter scans, and by more frequent switching between spacecraft and quasar. Only a slight improvement in the overall measurement accuracy can be obtained by increasing the measurement time beyond 1 hour in order to repeat the observations.

The following four scenarios are provided as examples of typical  $\Delta$ DOR measurements made by the DSN in the 2001 – 2003 time frame.

**2.1.4.1 Example 1, Spacecraft With One DOR Tone and Subcarrier Harmonics**

- Tone frequency: 19.1 MHz
- Subcarrier frequency: 375 kHz
- Number of channels: 4 spacecraft and 4 quasar
- Narrow channel bandwidth: 50 kHz sampled with 8-bit resolution
- Wide channel bandwidth: 2 MHz sampled with 2-bit resolution

Table 3. Channel Assignments for Example 1

Channel Pair	Spectral Component
1	Carrier
2	Upper 3 <sup>rd</sup> harmonic of subcarrier
3	Lower 1 <sup>st</sup> harmonic of DOR tone
4	Upper 1 <sup>st</sup> harmonic of DOR tone

**2.1.4.2 Example 2, Two Spacecraft With One DOR Tone and Subcarrier Harmonics**

- Tone frequency: 19.1 MHz
- Subcarrier frequency: 375 kHz
- Number of channels: 4 for each spacecraft and 8 quasar
- Narrow channel bandwidth: 50 kHz sampled with 8-bit resolution
- Wide channel bandwidth: 2 MHz sampled with 2-bit resolution

Table 4. Channel Assignments for Example 2

Channel Pair	Spectral Component
1	Carrier of spacecraft 1
2	Carrier of spacecraft 2
3	Upper 3 <sup>rd</sup> harmonic of spacecraft 1 subcarrier
4	Upper 3 <sup>rd</sup> harmonic of spacecraft 2 subcarrier
5	Lower 1 <sup>st</sup> harmonic of spacecraft 1 DOR tone
6	Lower 1 <sup>st</sup> harmonic of spacecraft 2 DOR tone
7	Upper 1 <sup>st</sup> harmonic of spacecraft 1 DOR tone
8	Upper 1 <sup>st</sup> harmonic of spacecraft 2 DOR tone

**2.1.4.3 Example 3, Spacecraft With Only Subcarrier Harmonics**

- Subcarrier frequency: 262 kHz
- Number of channels: 4 spacecraft and 4 quasar
- Narrow channel bandwidth: 50 kHz sampled with 8-bit resolution
- Wide channel bandwidth: 2 MHz sampled with 2-bit resolution

Table 5. Channel Assignments for Example 3

Channel Pair	Spectral Component
1	Carrier
2	Lower 30 <sup>th</sup> harmonic of subcarrier
3	Upper 26 <sup>th</sup> harmonic of subcarrier
4	Upper 30 <sup>th</sup> harmonic of subcarrier

In practice, squarewave subcarriers with finite risetimes have discrete spectral lines at the even harmonics of the subcarrier frequency whereas the odd harmonics may have data modulation. Therefore, even harmonics may be better choices for  $\Delta$ DOR assuming they have sufficient power. It also may be necessary to select even harmonics if the telemetry symbol rate cannot be reduced sufficiently to be processed by the  $\Delta$ DOR correlator.

**2.1.4.4 Example 4, Spacecraft With Uplinked Range Tone**

- Range Tone frequency: 1 MHz
- Number of channels: 3 spacecraft and 3 quasar
- Narrow channel bandwidth: 50 kHz sampled with 8-bit resolution
- Wide channel bandwidth: 2 MHz sampled with 2-bit resolution

Table 6. Channel Assignments for Example 4

Channel Pair	Spectral Component
1	Carrier
2	Lower 1 <sup>st</sup> harmonic of range tone
3	Upper 1 <sup>st</sup> harmonic of range tone

## 2.2 *Downlink Signal Structure and Power Allocation*

The target spacecraft may use one or two DOR tones, phase-modulated onto the downlink carrier, for a  $\Delta$ DOR measurement. The mathematical form of the downlink carrier may generally be modeled as

$$\sqrt{2P_T} \sin \left[ 2\pi f_c t + \theta d(t) + \phi_1 \sin(2\pi f_1 t) + \phi_2 \sin(2\pi f_2 t) \right] \quad (1)$$

where  $P_T$  is the total downlink power,  $f_c$  is the carrier frequency,  $d(t)$  is the telemetry and  $\theta$  its modulation index. The DOR tones will have frequencies  $f_1$  and  $f_2$ , and modulation indices of  $\theta_1$ , and  $\theta_2$  if two tones are present, however the second DOR tone will sometimes be absent.

### 2.2.1 *DOR Tones and Phase Ambiguity*

For each DOR tone that phase-modulates the downlink carrier, an upper and a lower fundamental harmonic are created. Thus, a (differential) group delay can be measured even when only one DOR tone modulates the carrier. However, it is sometimes advantageous to have two DOR tones. The DOR tones will normally be coherently related and may be coherently related to the carrier. Furthermore, if carrier-aided detection is to be used, the DOR tones must be coherently related to the carrier (Reference 4). If a DOR tone of about 20 MHz is used in the X band, then the downlink carrier must be assigned a channel very near the center of the allocated band, in order that the upper and lower fundamental harmonics of the DOR tone lie within the allocated band.

When two DOR tones are present, the purpose of the additional DOR tone is to resolve the phase ambiguity that is inherent in any range (or differential range) measurement. For example, in two-way sequential ranging, the phase ambiguity associated with the range clock is resolved by sequentially sending a set of range components of decreasing frequency, see module 203. With differential one-way ranging, the DOR tones are sent simultaneously rather than sequentially.

In order to make clear why two DOR tones are sometimes necessary, it is well to consider first the case of a single DOR tone. Corresponding to the single DOR tone, there are two fundamental harmonics (an upper and a lower). After each harmonic has been downconverted and recorded at the two stations, the differential phase between the two received copies of each harmonic may be plotted as indicated in Figure 3. The abscissa is the frequency of the observed harmonic as recorded at intermediate frequency. The ordinate is the differential phase. The column of points on the left side of Figure 3 represents the differential phase for the lower fundamental harmonic. The column of points on the right side of Figure 3 represents the differential phase for the upper fundamental harmonic. The horizontal separation between the two columns of points is the spanned bandwidth, which equals twice the frequency of the DOR tone. The slope of the line labeled "True" is the differential group delay for the DOR tone.

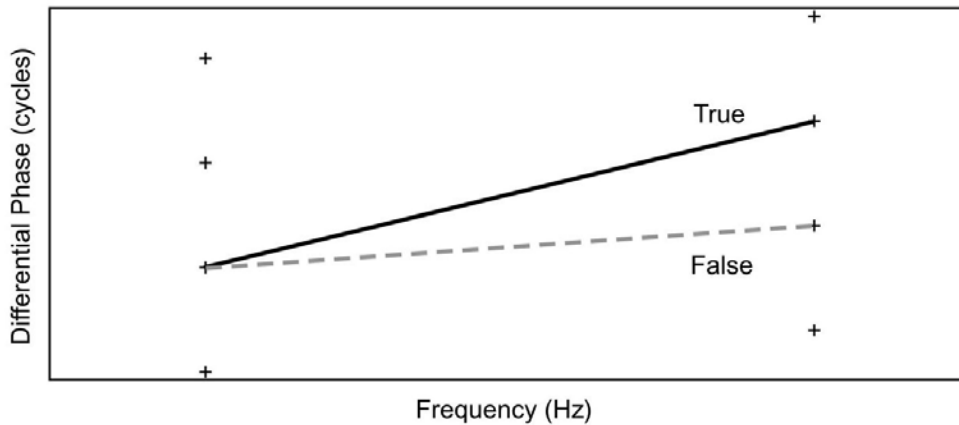


Figure 3. Phase Ambiguity with One DOR Tone

In Figure 3, there is a phase ambiguity since the DOR tone is a periodic signal. If the differential phase is regarded as having an integer number of cycles plus a fraction of one cycle, differential one-way ranging only measures the fractional part. That is why there is a column of points for the lower fundamental harmonic (and also for the upper fundamental harmonic). The points in each column are spaced by one cycle of phase. For the purpose of a  $\Delta$ DOR measurement, it is not necessary to determine which point in the first column of points represents the true differential phase for the lower fundamental harmonic. However, it is necessary to distinguish the true slope, representing the actual differential group delay, from the false slope shown as a dashed line in Figure 3. The difference between these two slopes equals the reciprocal of the spanned bandwidth. (There are other false slopes than the one shown in Figure 3, but these other false slopes have a value at least as far from the true slope as the reciprocal of the spanned bandwidth.) If the *a priori* knowledge of the differential group delay is good enough to rule out a false slope corresponding to a delay that differs from the true differential group delay by the reciprocal of the spanned bandwidth, then there is no need for a second DOR tone.

Figure 4 illustrates how differential group delay is determined when there are two DOR tones. The leftmost column of Figure 4 represents the differential phase for the lower fundamental harmonic of the higher-frequency DOR tone. The rightmost column represents the differential phase for the upper fundamental harmonic of the higher-frequency DOR tone. The middle columns represent differential phase for the lower and upper fundamental harmonics of the other (lower-frequency) DOR tone. The horizontal separation between the two outermost columns of points is the spanned bandwidth, which equals twice the frequency of the higher-frequency DOR tone. The true and false slopes shown in Figure 3 are reproduced in Figure 4. It is now clear how the second (lower-frequency) DOR tone helps resolve phase ambiguity. The true slope passes through legitimate points in the middle columns, whereas the false slope does not. On this basis, the false slope can be ruled out.



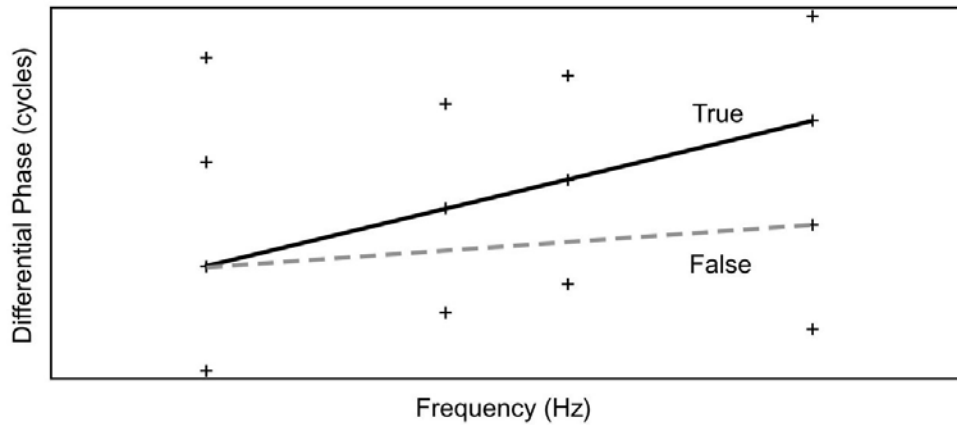


Figure 4. Resolution of Phase Ambiguity with a Second DOR Tone

It is important to use the largest possible spanned bandwidth because several measurement-limiting errors are inversely proportional to the spanned bandwidth, see Paragraph 2.4. When selecting DOR tone frequencies, however, it is necessary to consider the problem of ambiguity resolution. Ambiguity resolution requires two signal components that are not widely separated in frequency. These two goals, achieving a large spanned bandwidth and resolving the ambiguity, are not contradictory. Generally, one DOR tone frequency is selected large enough that the desired measurement accuracy can be achieved. It will often be the case that the reciprocal of twice this frequency is smaller than the uncertainty in the *a priori* knowledge of differential group delay. This need not be a problem. The ambiguity can still be resolved by including one or more of the following in the measurement: a second (lower-frequency) DOR tone, the residual carrier, or telemetry subcarrier harmonics. The choice of how many signal components to use must be carefully considered because every signal that modulates the carrier consumes link power and produces intermodulation products that waste link power.

### 2.2.2 Downlink Power Allocation

It will generally be necessary to determine the allocation of downlink power when one or two DOR tones share the downlink with telemetry. In describing the allocation of downlink power, it is useful to define functions  $\alpha(\theta)$  and  $\beta(\theta)$  as shown in Table 7.

Table 7. Definition of  $\alpha(\theta)$  and  $\beta(\theta)$  for  $\theta$  in peak radians

Telemetry type	$\alpha(\theta)$	$\beta(\theta)$
squarewave subcarrier or data only	$\cos(\theta)$	$\sin(\theta)$
sinewave subcarrier	$J_0(\theta)$	$\sqrt{2}J_1(\theta)$

### 2.2.2.1 *One DOR Tone*

When one DOR tone plus telemetry phase-modulate the downlink carrier, the allocation of downlink power is governed by the following equations. The ratio of residual-carrier power  $P_C$  to total power is

$$\frac{P_C}{P_T} = J_0^2(\phi_1) \cdot \alpha^2(\theta). \quad (2)$$

The ratio of telemetry data power  $P_D$  to total power is

$$\frac{P_D}{P_T} = J_0^2(\phi_1) \cdot \beta^2(\theta). \quad (3)$$

The ratio of the power  $P_1$  in one fundamental harmonic (upper or lower) of the DOR tone to the total power is

$$\frac{P_1}{P_T} = J_1^2(\phi_1) \cdot \alpha^2(\theta). \quad (4)$$

The modulation index  $\phi_1$  must be in units of radians, peak when substituted into the above equations. The above equations do not account for all downlink power. There is also power in higher harmonics of the DOR tone and in intermodulation products.

### 2.2.2.2 *Two DOR Tones*

When two DOR tones plus telemetry phase-modulate the downlink carrier, the allocation of downlink power is governed by the following equations. The ratio of residual-carrier power  $P_C$  to total power is

$$\frac{P_C}{P_T} = J_0^2(\phi_1) \cdot J_0^2(\phi_2) \cdot \alpha^2(\theta). \quad (5)$$

The ratio of telemetry data power  $P_D$  to total power is

$$\frac{P_D}{P_T} = J_0^2(\phi_1) \cdot J_0^2(\phi_2) \cdot \beta^2(\theta). \quad (6)$$

The ratio of the power in one fundamental harmonic (upper or lower) of a DOR tone to the total power is

$$\frac{P_1}{P_T} = J_1^2(\phi_1) \cdot J_0^2(\phi_2) \cdot \alpha^2(\theta) \quad (7)$$

for DOR tone 1, and

$$\frac{P_2}{P_T} = J_0^2(\phi_1) \cdot J_1^2(\phi_2) \cdot \alpha^2(\theta) \quad (8)$$

for DOR tone 2. The modulation indices  $\phi_1$  and  $\phi_2$  must be in units of radians, peak when substituted into the above equations. The above equations do not account for all downlink power. There is also power in higher harmonics of the DOR tones and in intermodulation products.

### 2.3 *DOR Tone Signal-to-Noise Spectral Density Ratio*

The signal-to-noise spectral density ratios of the DOR tones' fundamental harmonics are

$$\frac{P_i}{N_0} = \frac{P_i}{P_T} \cdot \frac{P_T}{N_0}, \quad i=1,2 \quad (9)$$

where  $P_T/N_0$  is the total downlink power-to-noise spectral density ratio. The ratios  $P_i/P_T$  are given in Paragraph 2.2.2.

The highest-frequency DOR tone sets the precision of the  $\Delta$ DOR measurement. This DOR tone is here labeled DOR tone 1. Its frequency is  $f_1$  and the power in each of its fundamental harmonics is  $P_1$ . The ratio  $P_1/N_0$  needs to be large enough that the contribution to  $\Delta$ DOR measurement error due to thermal noise is sufficiently small. The standard deviation of this error contribution, in units of time delay, is

$$\sigma_\tau = \frac{1}{2\pi\Delta f} \sqrt{\frac{1}{T_{\text{obs}}(P_1/N_0)_1} + \frac{1}{T_{\text{obs}}(P_1/N_0)_2}} \quad \text{sec}, \quad (10)$$

where  $T_{\text{obs}}$  is the observation (integration) time and  $\Delta f = 2f_1$  is the spanned bandwidth. The power-to-noise spectral density ratios for the DOR tone 1 fundamental harmonics at each of receiving stations 1 and 2 are denoted  $(P_1/N_0)_1$  and  $(P_1/N_0)_2$ . In the case where  $(P_1/N_0)_1 = (P_1/N_0)_2$ , which is usually a good approximation when both receiving stations have the same size aperture, Equation (10) reduces to

$$\sigma_\tau = \frac{\sqrt{2}}{2\pi\Delta f \sqrt{T_{\text{obs}} \cdot P_1/N_0}} \quad \text{sec}. \quad (11)$$

In addition,  $P_1/N_0$  must be large enough that the DOR tone 1 fundamental harmonics may be detected with confidence at each tracking station. This places the following constraint on  $P_1/N_0$  (Reference 5):

$$\frac{P_1}{N_0} \geq \begin{cases} 0.85, & \text{where } f_1 \text{ is a coherent sub - multiple of } f_c \\ 12.5, & \text{otherwise.} \end{cases} \quad (12)$$

The  $P_1/N_0$  required for detection is less when the DOR tone 1 frequency is a coherent sub-multiple of the residual-carrier frequency because the measured carrier frequency can, in this case, be used to aid in the detection of DOR tone 1. It is important to recall that  $P_1/N_0$  must also

be large enough to make the  $\Delta$ DOR measurement error contribution due to thermal noise sufficiently small.

The second DOR tone, if it is present, is used to resolve the phase ambiguity. This second DOR tone, labeled here as DOR tone 2, must have fundamental harmonics with a power-to-noise spectral density that is large enough for tone detection. Ordinarily, the frequency of the second DOR tone will be a coherent sub-multiple of the DOR tone 1 frequency, so

$$\frac{P_2}{N_0} \geq 0.85. \quad (13)$$

## 2.4 $\Delta$ DOR Measurement Error Models

There are a number of important error sources for  $\Delta$ DOR measurements. Models for these errors are given here. It is important to note that these models are based on the assumption that the measurements are in fact  $\Delta$ DOR, and not plain DOR. (Some of the following errors would be much larger for plain DOR, since common-mode errors would then not be canceled.) Units of time delay are employed here to characterize  $\Delta$ DOR measurement error.

Most of the time, a  $\Delta$ DOR measurement uses a quasar to define the reference direction. When this is the case, the error models given below may be used directly. In the exceptional case where a spacecraft with DOR tones serves to define the reference direction, the error contribution of Paragraph 2.4.2 (Receiver Noise in Quasar Detection) should be omitted and, instead, the error contribution of Paragraph 2.4.1 (Receiver Noise in DOR Tone Detection) should be included twice (once for each spacecraft). Also, the error contribution of Paragraph 2.4.3 should be interpreted as the error in knowledge of the reference spacecraft position. Finally, the error contribution of Paragraph 2.4.5 (Instrumental Phase Ripple) should be multiplied by  $\sqrt{2}$ , since two (statistically) equal errors are root-sum-squared together in this case.

The errors of  $\Delta$ DOR measurement can be very dramatically reduced if a spacecraft defines the reference direction and if this reference spacecraft and the target spacecraft are close enough (in an angular sense) to be served simultaneously by a common receive antenna. When a  $\Delta$ DOR measurement can be made under these circumstances, using two VLBI antennas, both simultaneously observing both spacecraft, this is called *Same-beam Interferometry*. Many of the error models given below either do not apply or must be drastically modified for the case of Same-beam Interferometry. For more information on this technique and the errors associated with it, the reader may wish to see References 1 and 6.

### 2.4.1 Receiver Noise in DOR Tone Detection

The first error source considered here is discussed above in Paragraph 2.3. It is the receiving system noise that is present while the DOR tones are being detected. Equation (10) gives the standard deviation of this error contribution as a function of the observation time,  $T_{\text{obs}}$ , the spanned bandwidth,  $\Delta f$ , and the power-to-noise spectral density ratios for the DOR tone 1 fundamental harmonics at each of receiving stations 1 and 2,  $(P_1/N_0)_1$  and  $(P_1/N_0)_2$ . When these two power-to-noise spectral densities are equal, Equation (11) may be used.

### 2.4.2 Receiver Noise in Quasar Detection

The receiving system noise that is present during quasar detection also contributes to  $\Delta$ DOR measurement error. The standard deviation (in units of time delay) for this error is

$$\sigma_\tau = \frac{1}{C_L 2\pi\Delta f} \sqrt{\frac{2T_{s1}T_{s2}}{T_{q1}T_{q2}WT_{\text{obs}}}} \text{ sec}, \quad (14)$$

where  $T_{\text{obs}}$  is the observation time,  $W$  is the passband bandwidth for each component of measured quasar signal,  $\Delta f$  is the spanned bandwidth, and  $C_L$  is a composite loss factor that includes the effects of system loss (Reference 5) and quantization loss.  $C_L$  has a value of 0.5 for 1-bit quantization, 0.7 for 2-bit quantization, and 0.8 for higher quantizations. The receiving system noise temperatures for the two receivers are denoted  $T_{s1}$  and  $T_{s2}$ . The equivalent temperatures at the two antennas due to radiation from the quasar are denoted  $T_{q1}$  and  $T_{q2}$ . These latter temperatures are related to the correlated source flux  $S_c$  (in janskys),

$$T_{qi} = 0.0003\pi\varepsilon_i r_i^2 S_c, \quad i = 1, 2 \quad (15)$$

where  $r_i$  and  $\varepsilon_i$  are the aperture radius (m) and efficiency of the  $i$ -th antenna.

### 2.4.3 Error in Knowledge of Quasar Position

In a  $\Delta$ DOR measurement, the angle to the spacecraft is measured relative to the position of a quasar. An error in the assumed position of the quasar leads to an error in the inferred position of the spacecraft. This error is given by (Reference 5),

$$\varepsilon_\tau = \frac{B_p}{c} \varepsilon_\theta \text{ sec}, \quad (16)$$

where  $\varepsilon_\theta$  is the angular position error in radians,  $c$  = speed of electromagnetic radiation in a vacuum in m/s, and  $B_p$  is the projection of the baseline onto a line that is perpendicular to the line-of-sight direction to the quasar (and in the plane formed by the baseline and the quasar). A typical value for  $\varepsilon_\theta$  is 1 nrad (References 7 and 8).

### 2.4.4 Clock Instability

Instability in the clocks and distributed frequency references at the stations lead to a  $\Delta$ DOR measurement error. This error is proportional to the time separating spacecraft and quasar observations,  $T_{\text{sep}}$  (Reference 5),

$$\varepsilon_\tau = 1.4 \times 10^{-14} T_{\text{sep}} \text{ sec}. \quad (17)$$

In Equation (17), the Allan deviation of the composite frequency and timing distribution has been assumed to be  $10^{-14}$ .

### 2.4.5 *Instrumental Phase Ripple*

When the DOR tones experience ripple in the phase response of the receiver instrumentation, this leads to a measurement error. This error is inversely proportional to the spanned bandwidth  $\Delta f$  (References 1 and 5),

$$\varepsilon_{\tau} = \frac{0.0028}{\Delta f} \text{ sec.} \quad (18)$$

In Equation (18), an instrumental phase ripple of 0.5 degree has been assumed.

### 2.4.6 *Error in Knowledge of Station Location*

In a  $\Delta$ DOR measurement, an error in the assumed positions of the stations leads to an error in the delay measurement. This error is proportional to the angular separation between the spacecraft and quasar (Reference 1),

$$\varepsilon_{\tau} = 5 \times 10^{-11} \Delta\theta \text{ sec,} \quad (19)$$

where  $\Delta\theta$  is the angular separation between the spacecraft and quasar, in units of radians. In Equation (19) an uncertainty in the baseline position coordinates of 1.5 cm has been assumed.

### 2.4.7 *Error in Knowledge of Earth Orientation*

In a  $\Delta$ DOR measurement, an error in assumed Earth orientation leads to an error in the delay measurement. This error is proportional to the angular separation between the spacecraft and quasar (Reference 1),

$$\varepsilon_{\tau} = \Delta\theta \frac{\varepsilon_{\text{UTPM}}}{c} \text{ sec,} \quad (20)$$

where  $\Delta\theta$  is the angular separation between the spacecraft and quasar in units of radians, and  $\varepsilon_{\text{UTPM}}$  is the positional uncertainty in universal time (UT1) and polar motion at the Earth's surface in units of meters (for  $c$  is in units of m/s). This error contribution and the previous error contribution (due to uncertainty of station location) have a similar dependence on  $\Delta\theta$ . Between these two error contributions, the error of Equation (20) dominates.

### 2.4.8 *Troposphere*

The uncertainty due to the variation in tropospheric delay causes the following error at each receiving station (References 1 and 5):

$$\varepsilon_{\tau} = 1.7 \times 10^{-11} \left| \frac{1}{\sin \gamma_{\text{sc}}} - \frac{1}{\sin \gamma_{\text{q}}} \right| \text{ sec.} \quad (21)$$

Here,  $\gamma_{\text{sc}}$  and  $\gamma_{\text{q}}$  are the elevation angles of the spacecraft and quasar as seen from the receiving station. There is an error of this type at each tracking station, and these two errors should be combined in a root-sum-square. In Equation (21) a zenith tropospheric delay uncertainty of 0.5 cm has been assumed.

### 2.4.9 *Ionosphere*

The uncertainty due to variation in the ionospheric delay causes the following composite error for the VLBI measurement (Reference 5):

$$\varepsilon_{\tau} = \frac{(20.6 + 23.9\Delta\theta) \times 10^9}{f_c^2} \text{ sec.} \quad (22)$$

As before,  $\Delta\theta$  is the angular separation between the spacecraft and quasar, in units of radians, and  $f_c$  is the carrier frequency in hertz. The error term of Equation (22) accounts for ionospheric error at both receiving stations.

### 2.4.10 *Solar Plasma*

The error due to scintillation acquired by the radio signals as they pass through the solar plasma is given by (Reference 5):

$$\varepsilon_{\tau} = \frac{1.8 \times 10^7}{f_c^2 (\sin \gamma_{\text{SEP}})^{1.3}} \cdot \left( \frac{B_p}{v_{\text{SW}}} \right)^{0.75} \text{ sec.} \quad (23)$$

As before,  $f_c$  is the carrier frequency in hertz and  $B_p$  is the projected baseline. The Sun-Earth-probe angle is denoted  $\gamma_{\text{SEP}}$ , and the solar wind velocity is  $v_{\text{SW}}$ . For consistency, if  $B_p$  is in kilometers, then  $v_{\text{SW}}$  will be in kilometers per second. The one term of Equation (23) accounts for the solar plasma scintillation induced on all radio signals to both receiving stations.

## 2.5 *$\Delta$ DOR Measurement Error Budget*

An example  $\Delta$ DOR error budget is shown in Table 8. The error is in time delay units (nsec). The overall error is 0.153 nsec in this example. The parameter values that were assumed in the compilation of this example error budget are shown in Table 9.

$\Delta$ DOR measurements with an accuracy of 0.12 nsec were realized with the 2001 Mars Odyssey mission (Reference 2). More recently, the Mars Exploration Rovers (MER) used  $\Delta$ DOR very successfully with a measurement error of about 0.04 nsec. The error budget of Table 8 should be considered conservative.

Table 8. Example  $\Delta$ DOR Error Budget

Error Source	Error (ns)
Receiver Noise (DOR Tones)	0.040
Receiver Noise (Quasar)	0.067
Quasar Position	0.027
Clock Instability	0.013
Instrumental Phase Ripple	0.073
Station Location	0.009
Earth Orientation	0.052
Troposphere	0.021
Ionosphere	0.088
Solar Plasma	0.003
Overall (root-sum-square)	0.153

Table 9. Parameter Values Associated with the Error Budget of Table 8

Parameter	Value
$\sigma_{\tau}$ (DOR tones)	0.040 ns
$\sigma_{\tau}$ (quasar)	0.067 ns
$\Delta f$	38.3 MHz
$T_{\text{sep}}$	15 minutes
$\Delta \theta$	10 degrees
$f_c$	8400 MHz
$\varepsilon_{\theta}$	1 nrad
$\gamma_{\text{SEP}}$	50°
$\gamma_{\text{sc}}$ (both antennas)	15°
$\gamma_{\text{q}}$ (both antennas)	20°
$B_p$	8000 km
$v_{\text{SW}}$	400 km/s



## ***References***

1. C. L. Thornton and J. S. Border, *Radiometric Tracking Techniques for Deep-Space Navigation*, Wiley-Interscience, Hoboken, NJ, 2003.
2. P. G. Antreasian, *et al.*, "2001 Mars Odyssey Orbit Determination During Interplanetary Cruise," *AIAA/AAS Astrodynamics Specialist Conference and Exhibit*, Monterey, CA, August 5-8, 2002.
3. S. A. Townes, *et al.*, "Operational Demonstration of Ka-Band Telecommunications for the Mars Reconnaissance Orbiter," *2003 IEEE Aerospace Conference*, Big Sky, MT, March 8-15, 2003.
4. Consultative Committee for Space Data Systems, *Radio Frequency and Modulation Systems*, CCSDS 401.0-B.
5. J. S. Border and J. A. Koukos, "Technical Characteristics and Accuracy Capabilities of Delta Differential One-Way Ranging ( $\Delta$ DOR) as a Spacecraft Navigation Tool," in Consultative Committee for Space Data Systems, *Report of the Proceedings of the RF and Modulation Subpanel 1E Meeting at the German Space Operations Centre: September 20-24, 1993*, CCSDS B20.0-Y-1, 1994.
6. J. S. Border, *et al.*, "Precise Tracking of the Magellan and Pioneer Venus Orbiters by Same-Beam Interferometry, Part I: Data Accuracy Analysis," *TDA Progress Report 42-110*, Jet Propulsion Laboratory, Pasadena, CA, August 15, 1992.
7. C. Ma, *et al.*, "The International Celestial Reference Frame as Realized by Very Long Baseline Interferometry," *The Astronomical Journal*, Vol. 116, pp. 516-546, July 1998.
8. C. Jacobs, *et al.*, "The JPL Extragalactic Radio Reference Frame: Astrometric Results of 1978-96 Deep Space Network VLBI," *TMO Progress Report 42-133*, Jet Propulsion Laboratory, Pasadena, CA, May 15, 1998.